Statistical speckle study to characterize scattering media: use of two complementary approaches

O. Carvalho[1*], B. Clairac[2], M. Benderitter[1], L. Roy[1]

[1]*Institut de Radioprotection et de Sureté Nucléaire, Département de Radio-Protection de l'Homme, 92262 Fontenay-aux-roses, France*
[2]*Laboratoire images, Signaux et Systèmes intelligents, Université de Paris XII Val-de-Marne, Créteil, France*
**Corresponding author: carvalho@univ-paris12.fr*

Abstract: Speckle produced by strongly-scattering media contains information about its optical properties. Statistical speckle study allows discrimination between media and enables one to characterize any change. Two approaches of the speckle phenomenon are used in the measurement of speckle produced by monodisperse-polystyrene microspheres in solution and mixtures of them: a stochastic approach based on the fractional Brownian motion and a classical frequential approach based on speckle size measurement. In this paper, we introduce an approach that contains the multi-scale aspect of the speckle; therefore it provides more information on the medium than the speckle dimension. The obtained results show that the stochastic approach allows a better samples discrimination than the classical frequential approach.

OCIS codes: (030.6140) Speckle; (290.5850) Scattering particle; (999.9999) Brownian motion; (170.0170) Medical optics and biotechnology

References and links

1. P. Lehmann, "Surface-roughness measurement based on the intensity correlation function of scattered light under speckle-pattern illumination," Appl. Opt. **38**, 1144-1152 (1999).
2. R. Berlasso, F. Perz Quintian, M. A. Rebollo, C. A. Raffo and N. G. Gaggioli, "Study of speckle size of light scattered from cylindrical rough surfaces," Appl. Opt. **39**, 5811-5819 (2000).
3. I. V. Fedosov and V. V. Tuchin, "The use of dynamic speckle field space-time correlation function estimates for the direction and velocity determination of blood flow," Proc. SPIE **4434**, 192-196 (2001).
4. D. A. Boas and A. G. Yodh, "Spatially varying dynamical properties of turbid media probed with diffusing temporal light correlation," J. Opt. Soc. Am. A **14**, 192-215 (1997).
5. J. D. Briers, G. Richard, and X. W. He, "Capillary blood flow monitoring using laser speckle contrast analysis (LASCA)," J. Biomed. Opt. **4**, 164-175 (1999).
6. D. A. Zimnyakov, J. D. Briers, and V. V. Tuchin, "Speckle technologies for monitoring and imaging of tissues and tissue like phantoms," Chap.18 in *Handbook of biomedical diagnostics*, Valery V. Tuchin, Ed. (SPIE press, Bellingham 2002).
7. J. W. Goodman, "Statistical Properties of Laser Speckle Pattern," in *Laser Speckle and Related Phenomena*, Vol. 9 in series Topics in Applied Physics, J.C. Dainty, ed., (Springer-Verlag, Berlin, Heidelberg New York Tokyo, 1984)
8. L. I. Goldfisher, "Autocorrelation function and power spectral density of last-produced speckle pattern," J. Opt. Soc. Am. A **55**, 247-253 (1964).
9. M. Françon, *Granularite Laser, speckle, application en optique*, Masson (Paris, 1978).
10. Q. B. Li and F. P. Chiang, "Three-dimensional of laser speckle," Appl. Opt. **31,** 6287-6291 (1992).
11. Y. Piederrière, F. Boulvert, J. Cariou, B. Le Jeune, Y. Guern, G. Le Brun, "Backscattered speckle size as a function of polarization : influence of particle-size and –concentration," Opt. Express **13**, 5030-5039 (2005).
12. Y. Piederrière, J. Le Meur, J. Cariou, J. F. Abgrall, and M. T. Blouch, "Particle aggregation monitoring by speckle size measurement; application to blood platelets aggregation," Opt. Express **12**, 4596-4601 (2004).
13. L. Zhifand, L. Hui, and Y. Qiu, "Fractal analysis of laser speckle for measuring roughness," Proc. SPIE **6027**, 470-476 (2006).

#84216 - $15.00 USD Received 18 Jun 2007; revised 1 Aug 2007; accepted 29 Aug 2007; published 5 Oct 2007

14. C. L. Benhamou, *et al*., "Fractal Analysis of radiographic Trabecular Bone Texture and Bone Mineral Density: Two Complementary Parameters Related to Osteoporotic Fractures," Journal Bone Miner. Res. **16**, 697–704 (2001).
15. L. Pothuaud, *et al*., "Fractal analysis of trabecular bone texture on radiographs: discriminant value in post menopausal osteoporosis," Osteoporos. Int. **8**, 618–625 (1998).
16. G. M. Tosoni, A. G. Lurie, A. E. Cowan, and J.A. Burleson, "Pixel intensity and fractal analyses: detecting osteoporosis in perimenopausal and postmenopausal women by using digital panoramic images," Oral Surgery, Oral Medicine, Oral Pathology, Oral Radiology, and Endodontology, **102**, 235-241 (2006).
17. T. Hyon Ha, *et al*. "Fractal dimension of cerebral cortical surface in schizophrenia and obsessive–compulsive disorder," Neurosci. Lett. **384**, 172-176 (2005).
18. S. Guyot, M. C. Péron, and E. Deléchelle, "Spatial Speckle Characterization by Brownian Motion analysis," Phys. Rev. E **70**, 046618 (2004).
19. J. W. Goodman, *Statistical Optics* (Wiley, New York, 1985), Chap. 4, pp. 124-127; Chap. 7, 340-350.
20. P. Abry, P. Gonçalves, and P. Flandrin, *Spectrum analysis and 1/f processes* (Springer, Berlin, 1995).
21. M. F. Barnsley, R.L. Devaney, B.B. Mandelbrot, H.-O. Peitgen, D. Saupe, and R. F. Voss, *The science of fractal images* (Springer, New-York, 1988).
22. T. D. Frank, A. Daffertshofer, PJ. Beek, "Multivariate Ornstein-Uhlenberg processes with mean field-dependent coefficients-application to postural sway," Phys. Rev. E **63**, (2001).
23. A. Pentland et al. "Fractal-based description of natural scenes," *IEEE Trans. Patt. Mach. Int.* **6**, No 6, 661–674 (1984).
24. H. Funamizu and J. Uozumi, "Generation of fractal speckles by means of a spatial light modulator," Opt. Express **15**, 7415-7422 (2007).
25. K. Uno, J. Uozumi, and T. Asakura, "Speckle clustering in diffraction patterns of random objects under ring-slit illumination," Opt. Commun. **114**, 203-210 (1995).
26. J. Uozumi, M. Ibrahim, and T. Asakura, "Fractal speckles," Opt. Commun. **156**, 350-358 (1998).
27. T. L. Alexander, J. E. Harvey, and A. R. Weeks, "Average speckle size as a function of intensity threshold level: comparison of experimental measurements with theory," Appl. Opt. **33**, 8240-8250 (1994).
28. C. F. Bohren, and D. R. Huffman, *Absorption and Scattering of Light by Small Particles*, (Wiley, New York, 1983).
29. B. Gelebart, *et al*., "Time- and space-resolved reflectance applied to the analysis of multi-layered turbid media," J. Opt. **28**, 234-244 (1997).
30. R. Simpson, *et al*., "Near-infrared optical properties of ex vivo human skin and subcutaneous tissues measured using the Monte Carlo inversion technique," Phys. Med. Biol. **43,** 2465-2478 (1998).
31. R.V. Hogg and J. Ledolter, *Engineering statistics*, (Macmillan Publishing Company, New-York, 1987).
32. D. A. Zimnyakov, V. V. Tuchin, and A. A. Mishin, "Spatial speckle correlometry in applications to speckle structure monitoring," Appl. Opt. 36, 5594-5607 (1997).
33. A. H. Hielscher, J. R. Mourant, and I. J. Bigio, "Influence of particle size and concentration on the diffuse backscattering of polarized light from tissue phantoms and biological cell suspensions," Appl. Opt. **36**, 125-135 (1997).

1. Introduction

For a long time, the speckle phenomenon was considered as a simple noise in imaging. However, speckle is a phenomenon which directly rises from the interaction of coherent light and medium. Therefore, the speckle statistical properties are related to the medium properties, and particularly to its optical properties. For this reason, since few years, physicists took an interest in the exploitation of the speckle and several applications have been developed: in stellar physics, in industry with the study of object roughness and deformation by spatial characteristics of the speckle [1, 2], or also in medical imagery. In this domain, correlometric methods [3,4] or laser speckle contrast measurement [5,6] can be used to analyse the motion of speckle field. Measurement of several spatial or dynamic characteristics of speckle can give much information for the medical diagnosis.

Goodman [7] and Goldfisher [8] were the first to study the statistical properties of the speckle using its Power Spectral Density and autocorrelation function. The first and second order statistics allow applications in imaging [9] and can be applied to explore the relationships between speckle dimension and experimental conditions [10]. Indeed, as speckle is produced by the interaction of coherent light/medium, any modification in the medium involves modification in the speckle statistic. Thus, several authors have studied effect of: scatterer size, their concentration or their aggregation, on speckle dimension [11, 12].

#84216 - $15.00 USD Received 18 Jun 2007; revised 1 Aug 2007; accepted 29 Aug 2007; published 5 Oct 2007

More recently, authors studied roughness effect of a standard rough surface on speckle statistic by a fractal approach [13]. Besides, fractal approach has been used to analyse biomedical images, for detection of osteoporotic fractures or of cerebral pathologies [14-17]. Authors in [18] have shown that speckle patterns, from monodisperse-polystyrene microspheres in solution, have been well described by the fractional Brownian motion theory.

Our interest is the application of the speckle statistical study to the dermatological domain, the complexity of application comes from the skin complexity. Looking to the works in [13-18], to complement a first analysis based on the speckle size measurement; the obtained results, from a fractal approach of speckle patterns produced by tissue phantoms composed of monodisperse-polystyrene microspheres in solution, are presented. Then, we opted to use the stochastic approach described in [18] for our speckle patterns analysis. In the purpose of using this approach in dermatological application, a backscattering configuration was used for our measurements.

In order to discriminate several scattering media, we propose to use a classical frequential approach based on the extraction of speckle size, and a fractal approach, based on the fractional Brownian motion statistic. A comparison between these two approaches is also presented. Three parameters can be extracted from the speckle pattern by this fractal approach: Hurst coefficient, the Saturation of the variance and the Self-similar element. These parameters characterize the speckle pattern at three different scales, then they can give complementary information about the medium and about its modifications than speckle dimension. Our samples consist on tissue phantoms composed of monodisperse-polystyrene microspheres in solution of deionised water and mixtures of them. As in biological tissues there is an extreme optical complexity due to the presence of several biological structures of various sizes (from about 0.01 µm to 10 µm), six different sizes of microspheres were used in this interval. In order to investigate the effect of the scatterer sizes and of their size distribution on these statistical parameters, we study the backscattered speckle from samples containing each microsphere diameter and mixtures of them. In Section 2, the speckle statistical theory and the frequential classical approach used are recalled. In Section 3, we recall the speckle approach by the fractional Brownian motion evoked by [18]. Our experimental setup is presented in Section 4. Section 5 concerns the obtained results for our tissue phantoms that are discussed in Section 6. Our conclusion is in Section 7.

2. Speckle statistics

2.1 Statistic of 1st order

Let us consider a backscattered coherent light by a rough surface. For each spot in space, the electric field amplitude corresponds to the sum of all contributions of illuminated points:

$$A(x,y,z)=\frac{1}{\sqrt{N}}\sum\left|a_k\right|\exp(j\varphi_k) \tag{1}$$

where N is the scatterers number, a_k and φ_k the amplitude and the phase of the k^{th} contribution, respectively.

This amplitude appears as a random walk in a complex plan. Moreover, the following hypotheses are considered:

(i) The amplitude a_k and phase φ_k of the k^{th} contribution are independent between them and of other contribution.

(ii) The phases φ_k are uniformly distributed on $[0;2\pi]$.

From these hypotheses, Goodman [7] developed the probability density function for the real and imaginary parts of the field. The amplitude has a circular Gaussian distribution:

$$P\left(A^{(r)},A^{(i)}\right)=\frac{1}{2\pi\sigma^2}\exp\left\{-\frac{[A^{(r)}]^2+[A^{(i)}]^2}{2\sigma^2}\right\} \tag{2}$$

#84216 - $15.00 USD Received 18 Jun 2007; revised 1 Aug 2007; accepted 29 Aug 2007; published 5 Oct 2007

where $\sigma^2 = \lim_{N\to\infty}\left\{\inf \frac{1}{N}\sum_{k=1}^{N}\frac{\left\langle |a_k|^2 \right\rangle}{2}\right\}$ and $\langle\ \rangle$ is the spatial average.

Hence, the probability density function of the intensity I can be expressed by:

$$P(I) = \frac{1}{2\sigma^2}\exp\left(-\frac{I}{2\sigma^2}\right) \tag{3}$$

However, the observed intensity is that detected by the camera. Therefore, it corresponds to the spatio-temporal integration of the absolute intensity. Thus, the probability density function of the intensity detected I_d is [19]:

$$P(I_d) = \left(\frac{M}{\langle I_d \rangle}\right)^M \frac{{I_d}^{M-1}}{\Gamma(M)}\exp\left(-\frac{M.I_d}{\langle I_d \rangle}\right) \tag{4}$$

where Γ is the Gamma function, $M = \langle I_d \rangle^2 / {\sigma_I}^2$ and ${\sigma_I}^2$ the variance of the intensity. M can be interpreted as the number of speckle grains detected. For M = 1, this probability density corresponds to be a function in exponential decrease and tends to be a Gaussian distribution when $M\to\infty$. Experimentally, it tends to a Gaussian distribution when $M >> 1$ [19].

2.2 Statistic of 2nd order

The Power Spectral Density (PSD) of a signal is defined by the module square of its Fourier transform (denoted *FT*). Then, the PSD of the intensity is:

$$PSD(I(x,y)) = \left|FT(I(x,y))\right|^2 \tag{5}$$

The autocorrelation function of the intensity at two points (x_1, y_1) and (x_2, y_2) in the observation plane (x, y) is defined as follow:

$$R_I(\Delta x, \Delta y) = \langle I(x_1, y_1) I(x_2, y_2) \rangle \tag{6}$$

where $\Delta x = x_1 - x_2$ and $\Delta y = y_1 - y_2$. If $x_2 = 0$, $y_2 = 0$, $x_1 = x$ and $y_1 = y$ we can write:

$$R_I(\Delta x, \Delta y) = R_I(x, y) \tag{7}$$

According to the theorem of Wiener-Khintchine, the autocorrelation function of the intensity is given by the inverse Fourier transform (denoted FT^{-1}) of the *PSD* of the intensity:

$$R_I(x,y) = FT^{-1}\left[PSD(I(x,y))\right] \tag{8}$$

The normalized autocovariance function of the intensity, denoted $c_I(x,y)$, corresponds to the normalized autocorrelation function with a zero base and provides a reasonable measurement of the "average width" of a speckle [7]:

$$c_I(x,y) = \frac{R_I(x,y) - \langle I(x,y) \rangle^2}{\langle I(x,y)^2 \rangle - \langle I(x,y) \rangle^2} \tag{9}$$

#84216 - $15.00 USD Received 18 Jun 2007; revised 1 Aug 2007; accepted 29 Aug 2007; published 5 Oct 2007

According to Eq. (5), Eq. (8) and Eq. (9), the normalized autocovariance function of the intensity can be calculated from the intensity distribution of the measured speckle:

$$c_I(x,y) = \frac{FT^{-1}\left(\left| FT\left(I(x,y)\right)\right|^2 \right) - \left\langle I(x,y)\right\rangle^2}{\left\langle I(x,y)^2\right\rangle - \left\langle I(x,y)\right\rangle^2} \tag{10}$$

$c_I(x,0)$ and $c_I(0,y)$ correspond to the horizontal and the vertical profiles of $c_I(x,y)$, respectively. Their width at half maximum are denoted dx and dy, respectively. Figure 1 shows the horizontal profile $c_I(x,0)$ of the normalized autocovariance function $c_I(x,y)$.

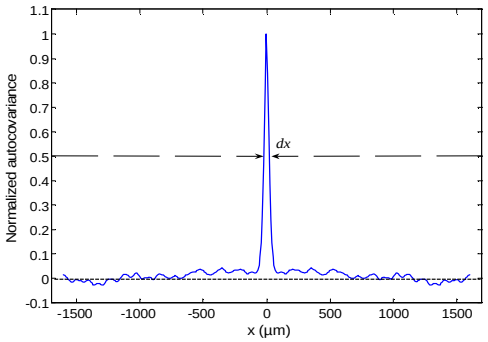

Fig. 1. Normalized autocovariance function $c_I(x,0)$, from speckle pattern of Fig. 4(b). dx is the width at half maximum.

dx and dy give the "average width" of speckle grains in the two dimensions of the image and they constitute the "speckle size". The well known classical frequential approach of the phenomenon speckle is based on this statistical property. This approach allows to characterize spatially the speckle pattern through the characteristic of these grains.

3. Fractional Brownian motion (fBm) applied to the speckle phenomenon: diffusion equation of the speckle pattern

The increment of a process X such as a Brownian motion is described by:

$$\left\langle \left[X(t+\Delta t) - X(t)\right]^2 \right\rangle \propto \Delta t \tag{11}$$

Where t is the time, Δt is the time increment and $\propto$ is the proportional sign.
In [18], the authors show the correlation between statistics of the speckle and statistics of the Brownian motion. Indeed, the speckle theory supposes that there is no-correlation between the amplitudes and phases and between their increments. From a signal processing point of view, the amplitudes of the speckle correspond to a white Gaussian noise. As the Brownian motion process is the time integration of the white Gaussian noise, the intensities detected of the speckle correspond to a Brownian motion. Therefore, their first order statistics have the same nature: Gaussian for the amplitude and for the intensity distributions. Figure 2 shows the PSD of a) several experimental speckle patterns and b) of the speckle pattern shown in Fig. 4(b), in log-log scale, where a decrease in $1/f^{\beta}$ (where $\beta \in [0,1]$) is observed for high frequencies. This behaviour in power law is characteristic of a self-similar process [20]. Consequently, the second order statistics of the observed speckle and of the Brownian motion have also the same characteristics: their PSD present a decrease in $1/f^{\beta}$ and their increments are Gaussians in the both cases.

#84216 - $15.00 USD Received 18 Jun 2007; revised 1 Aug 2007; accepted 29 Aug 2007; published 5 Oct 2007

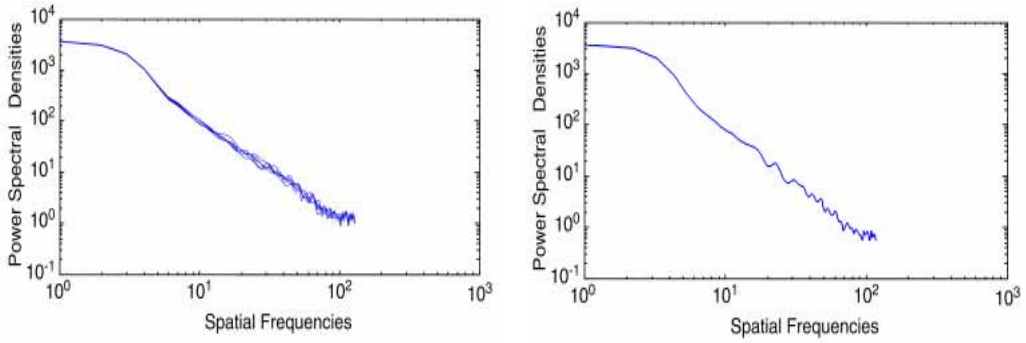

a) b)

Fig. 2. Power Spectral Density of a) experimental speckle patterns and b) of speckle pattern of Fig. 4(b) (log-log scale).

Nevertheless, this similitude with the Brownian motion has also some divergences [18]. The optical properties of the medium are not taken into account in the speckle statistic, which can explain these divergences. For this reason, a generalization with the fractional Brownian motion was considered. In the stochastic theory of the Brownian motion, Eq. (11) corresponds to the increment process of the fractional Brownian motion if $H = 0.5$. Indeed, the increment process of the fractional Brownian motion is expressed as follow:

$$\left\langle \left[X(t+\Delta t) - X(t) \right]^2 \right\rangle \propto \Delta t^{2H} \tag{12}$$

where $H \in [0,1]$ is the Hurst coefficient that reflects the Hölderian regularity in each point of the trajectory [21]. Equation (12) is known as the diffusion function of the process X. In fact, the fractional Brownian motion is the generalization of the Brownian motion. For the Brownian motion, there is no correlation between the increment because $H = 0.5$ [20].

To describe the diffusion function of the speckle pattern, it is necessary to express its increment process for the intensity in the space scale. For the horizontal direction y of the speckle pattern, with the hypothesis of stationarity for the second order, we obtain:

$$\left\langle \left[I(x+\Delta x, y) - I(x,y) \right]^2 \right\rangle = 2\left(\left\langle I(x,y)^2 \right\rangle - \left\langle I(x+\Delta x, y) I(x,y) \right\rangle \right) \tag{13}$$

then:

$$\left\langle \left[I(x+\Delta x, y) - I(x,y) \right]^2 \right\rangle = 2\left(\left\langle I(x,y)^2 \right\rangle - C_{ff} \right) \tag{14}$$

where C_{ff} is the autocorrelation function of the speckle pattern intensity I and $\left\langle I(x,y)^2 \right\rangle = {\sigma_I}^2 + \left\langle I(x,y) \right\rangle^2$.

The decrease of the speckle PSD for high frequencies characterizes local regularity for the trajectories of the process. From the fractal theory [20], a process X which presents local regularity is described for its autocorrelation function by:

$$C_{ff} = \left\langle X(t) X(t+\Delta t) \right\rangle = \sigma^2 \exp\left(-\lambda \left| \Delta t \right|^{2H} \right) \tag{15}$$

Hence, from Eq. (14) and Eq. (15) and after centering the process, the diffusion equation of the speckle pattern for every horizontal dimension y, is [18]:

#84216 - $15.00 USD Received 18 Jun 2007; revised 1 Aug 2007; accepted 29 Aug 2007; published 5 Oct 2007

$$\left\langle \left[I(x+\Delta x, y) - I(x, y) \right]^2 \right\rangle = 2{\sigma_I}^2 \left(1 - \exp\left(-\lambda \left| \Delta x \right|^{2H} \right) \right) \tag{16}$$

then:

$$\log\left(\left\langle \left[I(x+\Delta x, y) - I(x, y) \right]^2 \right\rangle \right) = \log\left(2{\sigma_I}^2 \right) + \log\left(1 - \exp\left(-\lambda \left| \Delta x \right|^{2H} \right) \right) \tag{17}$$

Three parameters can be extracted from this equation:

- *H*, the Hurst coefficient, is related to the image fractal dimension D_f according to the expression $D_f = d + 1 - H$, where *d* is the topologic dimension. When $H \to 1$, then $D_f \to d$; therefore we tend towards a perfect regular image, in the "Hölderian" sense. *H* characterizes the image at a local scale. Then, it is a characteristic of speckle grains. Indeed, it can be easily shown that, if $\Delta x << \lambda$ *i.e.* at a local scale in the speckle pattern and for $H > 0{,}5$, the Eq. (17) can be written like: $\log\left(\left\langle \left[I(x+\Delta x, y) - I(x, y) \right]^2 \right\rangle \right) \propto 2H \log(\Delta x)$. We can note the analogy with the increment process of the fractional Brownian motion [Eq. (12)].
- *S*, the Self-similar element, given by π / λ [22], allows the quantization of the dimension in the image that separates the classic from the self-similarity properties of the speckle. In this dimension, the process is scale invariant.
- *G*, the Saturation of the variance equal to $2{\sigma_I}^2$, characterizes the image at a global scale.

For a speckle pattern and for every horizontal dimension *y*, the intensity increments $f(x) = \log\left(\left\langle \left[I(x+\Delta x, y) - I(x, y) \right]^2 \right\rangle \right)$ are calculated and approximated according to Eq. (17) by:

$$\left\| f(x) - \left[a + \log\left(1 - \exp\left(-b \left| \Delta x \right|^c \right) \right) \right] \right\|_2^2 \le \varepsilon \tag{18}$$

where $\varepsilon = 10^{-5}$ is a mean square error. We can identify then the three coefficients a, b, c according to Eq. (17):

$$\begin{cases} a = \log(2\sigma_I^2) \\ b = \lambda \\ c = 2H \end{cases} \tag{19}$$

Speckle pattern is treated row by row or column by column. The diffusion curve of one speckle pattern corresponds to the mean of all diffusion curves, for each dimension in the image. This model allows a good fitting of our speckle patterns, as we can see in Fig. 4(a).

Figure 3(a) illustrates the obtained fitting results using the procedure based on Eq. (18) (arbitrary unity), in this example the measured diffusion curve is that of the homogeneous synthetic speckle pattern shown in Fig. 3(b). The periodic structure of this homogeneous image can be seen in its diffusion curve that explains the bad obtained fitting results in the far neighborhood. Nevertheless, in this case, Hurst coefficient is equal to 1, which is the accepted value for a regular image at the Hölderian sense [21]. This result confirms than *H* can be considered as a regularity parameter.

#84216 - $15.00 USD Received 18 Jun 2007; revised 1 Aug 2007; accepted 29 Aug 2007; published 5 Oct 2007

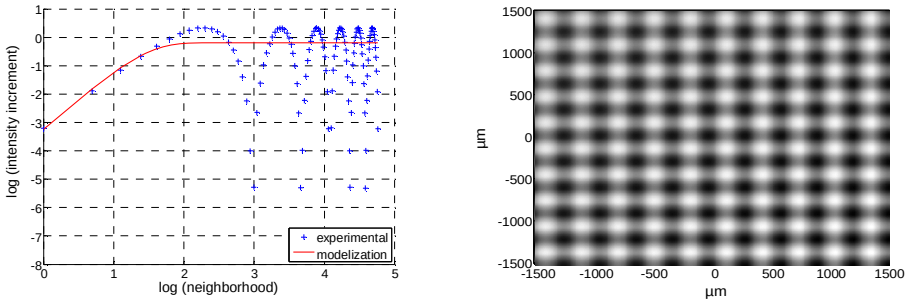

a) b)

Fig. 3. Speckle diffusion function a) from synthetic speckle pattern b).

Figure 4 presents a graphical representation of Eq. (18) (arbitrary unity) that allows a good fitting of the speckle pattern diffusion curve, obtained from scattering medium composed of monodisperse-polystyrene microspheres of 0,20 µm diameter, in solution of deionised water. Then, the three parameters of Eq. (18) can be extracted using Eq. (19). We can note that the *H* value found is lower than 1 (≈ 0,77, see Section 5) that means that this speckle pattern is more rough than that of Fig. 3(b) in the Hölderian sense, this can be appreciate through the comparison of Fig. 3(b) and Fig. 4(b).

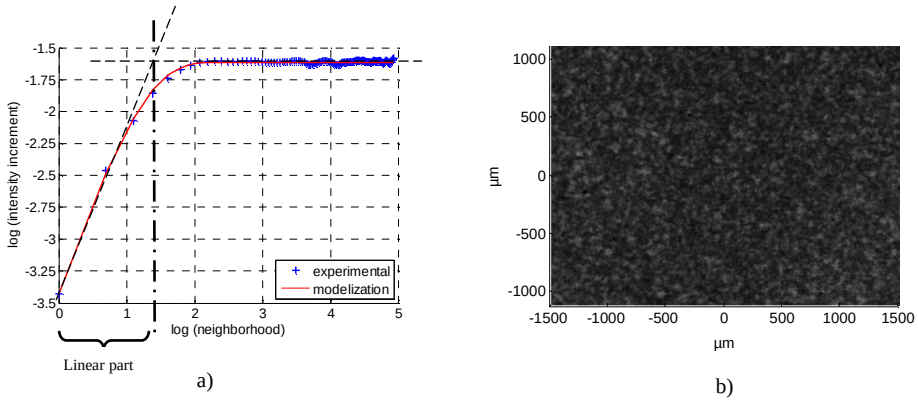

a) b)

Fig. 4. Speckle diffusion function a) from speckle pattern b) obtained by monodisperse-polystyrene microspheres in solution of deionised water (0, 20-µm microspheres).

Among many methods that can extract the information from natural images, fractal methods are the efficient candidates [14-17, 23] and fractional Brownian motion is widely used. In this paper, we use the stochastic approach of the fractional Brownian motion to characterize speckle patterns obtained from samples composed of polystyrene-microspheres in solution in backscattering configuration. The fractional Brownian motion has fractal properties because of its self-similarity behaviour. This property was found from our samples studied in this paper. Indeed, the Fig 2(b) shows a decrease in $1/f^{\beta}$ in the speckle pattern PSD produced from microspheres of 0, 20 µm diameter. The decrease in $1/f^{\beta}$ is the characteristic of a self-similar process [20]. As we can see in Fig. 4, this power law behaviour was also found in the diffusion curve of a speckle pattern from our sample, at local spatial neighborhood, in the same range of 1-2 decades. This property is observed in the speckle PSD in case of "fractal speckle" (speckle having fractal properties produced from fractal objects) [24]. Usually, fractal speckle is observed from fractal object [24-26] but for a medium

#84216 - $15.00 USD Received 18 Jun 2007; revised 1 Aug 2007; accepted 29 Aug 2007; published 5 Oct 2007

composed of monodisperse-polystyrene microspheres in solution, there is no proof that it is has fractal properties. Then we can not call the speckle observed in this study "fractal speckle". Nevertheless, authors in [25, 26] have observed speckle patterns having fractal properties from non-fractal object in case of diffuser illuminated with a ring-slit aperture. Other authors have also observed speckle patterns having fractal properties in case of polystyrene-microspheres in solution illuminated in backscattering configuration [18] and in case of metallic standard rough surface also illuminated in backscattering configuration [13]. In these two last cases, the experimental setup used is the analogue to that we used in this study. In [13], authors showed the self-similarity behaviour in the structure of speckle patterns produced from metallic standard rough surface and they compared the fractal dimension of the speckle pattern with the surface roughness and different style of them. Looking to all these references and to our observations, we considered that we can apply a fractal approach to analyse speckle patterns observed from our samples studied through the fractional Brownian motion theory.

4. Experimental setup and methods

Figure 5 illustrates the experimental setup to observe backscattering speckle produced by polystyrene microspheres in solution of deionised water. A non polarized HeNe laser illuminates at 632.8 nm the scattering medium with an intensity power of 15 mW. The speckle produced is recorded by a CCD camera containing 384 × 288 pixels of size 8 µm × 8 µm.

The sample observed is scatters in solution; then, we have mobility in the medium. Therefore, a random agitation of the speckle intensity is observed which is called "boiling speckle" and corresponds to the speckle intensity fluctuations. To avoid recording this blurred speckle, we must choose a time exposure of the camera shorter than the time scale of these fluctuations [6]. We chose the shorter image acquisition time provided by our camera of 10^{-4} s, which is shorter than the correlation times measured for our samples. For each sample under study, 200 speckle patterns were recorded with 25 Hz frequency and were digitized with an 8-bit precision by the analog-to-digital converter.

Speckle size is increasing with the distance L between the surface of the medium and the CCD camera [10]. To have a good statistical evaluation of the speckle pattern, we must have many speckle grains in the image. Furthermore, the size of speckle grains must be larger compared to the pixel size of the CCD array [27]. In order to respect both conditions, we set the CCD camera at a distance L = 20 cm from the surface of the medium.

The CCD camera, the laser and the sample are placed in the vertical plane. In order not to record specular reflections from the sample surface, the HeNe laser was positioned at an angle $\psi = 25°$ with the CCD camera.

The monodisperse-polystyrene microspheres are provided in solution with deionised water from Polyscience Inc. (Germany). Six different diameters of microspheres: 0.20, 0.50, 0.75, 1.00, 1.50, and 2.00 µm were used to have several samples under study. N_0 is the initial concentration defined as the number per cubed meter. For polystyrene microspheres and at the wavelength used here, the absorption can be omitted regarding the scattering effect. By dilution in deionized water, we can adjust their concentration c to obtain the scattering coefficient μ_s required, according to Mie theory [28]. Table 1 presents the initial number of particles per cubed meter N_0 and scattering parameters issued from Mie calculation for each microsphere diameter d: the scattering coefficient μ_s with respect to c, the scattering efficiency factor Qs and the anisotropy factor g. The reduced scattering coefficient μ_s' introduced as the equivalent isotropic scattering coefficient of an otherwise anisotropically-scattering medium is also presented.

#84216 - $15.00 USD Received 18 Jun 2007; revised 1 Aug 2007; accepted 29 Aug 2007; published 5 Oct 2007

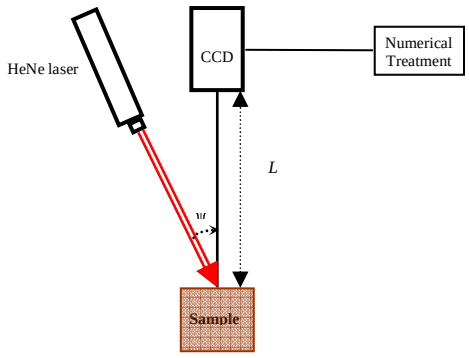

Fig. 5. Experimental setup (Face view).

Table 1. Scattering coefficient with respect to *c*, scattering efficiency factor and anisotropy factor of polystyrene microspheres (Mie Calculation). *c* can be adjusted to obtain μ_s required.

d (µm)	N_0 (m^{-3}) (*c* = 100%)	μ_s (cm^{-1})	*Qs*	*g*	$\mu_{s'}$ (cm^{-1}) = $\mu_s(1-g)$
0.20	5.68×10^{18}	2.85 *c*	0.16	0.325	1.92 *c*
0.50	3.64×10^{17}	5.42 *c*	0.76	0.825	0.95 *c*
0.75	1.08×10^{17}	7.21 *c*	1.51	0.896	0.75 *c*
1.00	4.55×10^{16}	8.14 *c*	2.28	0.92	0.65 *c*
1.50	1.35×10^{16}	7.48 *c*	3.15	0.934	0.49 *c*
2.00	5.68×10^{15}	4.97 *c*	2.78	0.92	0.40 *c*

In this paper, we are interested by the application on dermatological pathologies to discriminate healthy versus pathological skin, the first objective of our experiments on several media is to be able to discriminate them.

In order to see the effect of the scatters size on speckle statistic, the concentration *c* of all microspheres sizes have been adjusted to have the same scattering coefficient μ_s. In biological tissues and for the therapeutic window (about 600 nm -1000 nm), the scattering coefficient varies from 100 cm^{-1} to 500 cm^{-1} [29]. Furthermore, authors in [30] have determined *ex vivo* at λ= 633 nm by reflectance and transmittance measurements, the scattering coefficient on samples of human skin. They obtained mean values for μ_s about 126 cm^{-1} for the underlying fat layer dermis and 273 cm^{-1} for Caucasian dermis. Therefore, we chose a scattering coefficient value of μ_s=180 cm^{-1}.

In biological tissues we have an extreme optical complexity due to the presence of several biological structures of various sizes (from about 0.01 µm to 10 µm). Therefore, in order to obtain a sample which could simulate the real biological skin, all the sizes of microspheres in solution were mixed with a volume fraction of 1/6 for each. To see the effect of the distribution in smaller particles in this mixture, the measurements were also carried out by addition in this mixture of smaller microspheres, four times successively under different volume ratios. The same procedure is carried out for addition of larger microsphere:

i. mixture *m*: all size microspheres with a volume fraction f_v of 1/6 for each diameter. Two mixtures *m* were carried out for each microspheres addition type.
ii. mixture *m*(3:1): composed of mixture *m* supplemented with 0.20 µm (or 2.00 µm) in volume ratio (3:1).

#84216 - $15.00 USD Received 18 Jun 2007; revised 1 Aug 2007; accepted 29 Aug 2007; published 5 Oct 2007

iii. mixture *m*(3:2): composed of mixture *m* supplemented with 0.20 μm (or 2.00 μm) in volume ratio (3:2).
iv. mixture *m*(1:1): composed of mixture *m* supplemented with 0.20 μm (or 2.00 μm) in volume ratio (1:1).

5. Results

In the first phase, we studied the effect of the microspheres sizes on the speckle size and on the model parameters described above. In the second phase, we studied the microspheres size distribution effect on these parameters, either for the smaller (0.20 μm) or for the larger (2.00 μm) microspheres in a mixture of all particle diameters.

We chose to treat the horizontal direction of the image which contains the higher number of pixels. From each sample under study, we have a great size of sample (n = 200), then to emphasize discrimination between our samples under study (groups), we made an analysis of variance by the ANOVA test [31]. We define the parameter *p*, the p-value for the null hypothesis H_0, corresponding to the variability between groups. Nevertheless, the ANOVA tests the hypothesis that all groups are statically the same against the general alternative that they are not all the same. If the global null hypothesis H_0 is rejected and in order to know which pairs of groups are significantly different, and which are not, we used a "Multiple Comparison test". From each sample under study as described in Section 4, and for each of 200 speckle patterns recorded by the CCD camera, we calculated, the speckle size from the spatial autocorrelation function described in Subsection 2.2, and the model parameters according to the procedure described in Section 3. We deduced then the corresponding mean and standard deviation values.

4.1 Influence of microspheres sizes on speckle statistic: classical frequential and fractal approach.

We calculated speckle size and model parameters for each microsphere diameter. Results are showed in Table 2 and Fig. 6.

Table 2. Speckle size *dx* and model parameters (Saturation of the variance *G*, Self-similarity *S*, and Hurst coefficient *H*) for each microsphere diameter *d*.

d (μm)	0.20	0.50	0.75	1.00	1.50	2.00
dx (μm)	37.03±1.00†	22.43±0.51†	18.21±0.20†	16.18±0.16	16.07±0.14	16.12±0.12
G	0.200±0.016†	0.238±0.021†	0.276±0.022	0.269±0.020†	0.277±0.020	0.288±0.022†
S	17.53±0.32†	8.56±0.23†	5.90±0.06†	5.01±0.05†	4.63±0.04†	5.29±0.05†
H	0.768±0.007†	0.796±0.010†	0.835±0.008†	0.863±0.010†	0.874±0.010†	0.841±0.009†

† = discrimination with $p < 0.01$.

For the *length dx* and with a p-value less than 0.01, we have discrimination between all miscrosphere diameters except between 1.00, 1.50 and 2.00 μm. For Hurst coefficient *H*, and Self-similarity *S*, we have a very good discrimination between all diameters with a p-value $p << 0.01$. The Saturation of the variance *G*, discriminates all microsphere diameters except for 0.75 and 1.50 μm.

#84216 - $15.00 USD Received 18 Jun 2007; revised 1 Aug 2007; accepted 29 Aug 2007; published 5 Oct 2007

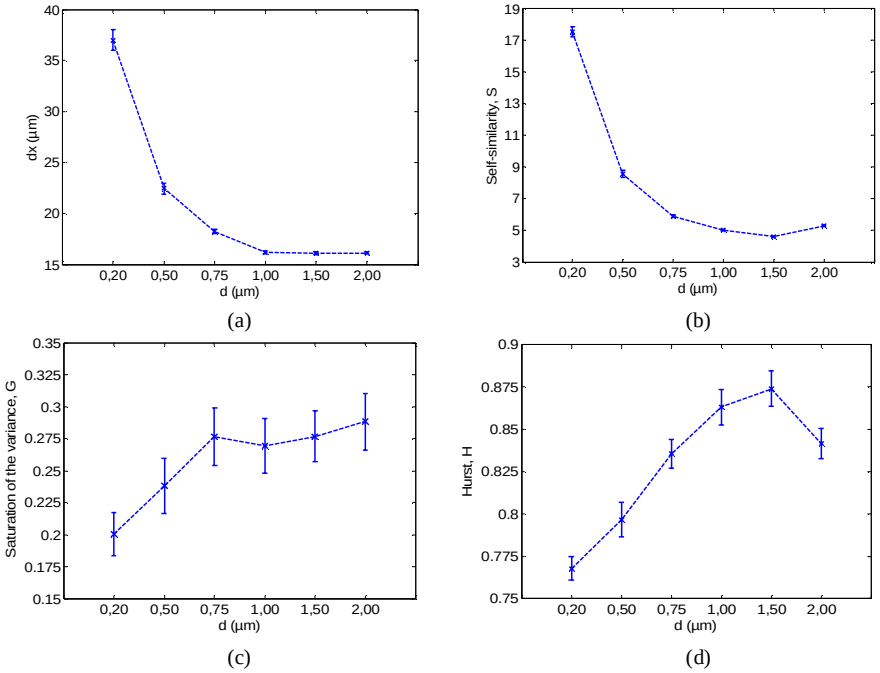

Fig. 6. Evolution of speckle size *dx* (a) and model parameters (Self-similarity *S* (b), Saturation of the variance *G* (c) and Hurst coefficient *H* (d)) versus the microsphere diameter *d*.

4.2 Influence of the size distribution of smaller and larger microspheres on speckle statistic: classical frequential and fractal approach.

We calculated speckle size and model parameters on several mixtures of microspheres as described in Section 4. Results for each mixture are shown in Table 3 and Fig. 7.

Table 3. Speckle size *dx* and model parameters (Saturation of the variance *G*, Self-similarity *S*, and Hurst coefficient *H*) for each mixture. Mixture *m* corresponds to a mixture with a volume fraction f_v =1/6 for each microsphere size, mixture *m*(3:1), *m*(3:2) and *m(1:1)* correspond to the mixture *m* supplemented with smaller (0.20 µm) or larger microspheres (2.00 µm) with a ratio of (3:1), (3:2) and (1:1), respectively.

Mixture	*m*		*m*(3:1)		*m*(3:2)		*m*(1:1)	
Microsphere addition	none	none	0.20 µm	2.00 µm	0.20 µm	2.00 µm	0.20 µm	2.00 µm
dx (µm)	20.28 ± 0.22†	20.82 ± 0.19‡	24 ± 0.28†	18.82 ± 0.18‡	26.07 ± 0.34†	18.11 ± 0.18	28.19 ± 0.42†	18.08 ± 0.16
G	0.230 ± 0.020†	0.236 ± 0.020	0.214 ± 0.017	0.239 ± 0.022	0.204 ± 0.016†	0.243 ± 0.022‡	0.210 ± 0.017	0.25 ± 0.024‡
S	7.51 ± 0.17†	7.31 ± 0.13‡	9.86 ± 0.17†	6.75 ± 0.11‡	11.27 ± 0.21†	6.53 ± 0.11‡	12.79 ± 0.23†	6.36 ± 0.08‡
H	0.789 ± 0.011†	0.794 ± 0.010‡	0.773 ± 0.008†	0.804 ± 0.010‡	0.766 ± 0.008	0.807 ± 0.010‡	0.765 ± 0.010	0.811 ± 0.010‡

†,‡ = discrimination with $p < 0.01$; †: for addition of 0.20 µm; ‡: for addition of 2.00 µm.

#84216 - $15.00 USD Received 18 Jun 2007; revised 1 Aug 2007; accepted 29 Aug 2007; published 5 Oct 2007

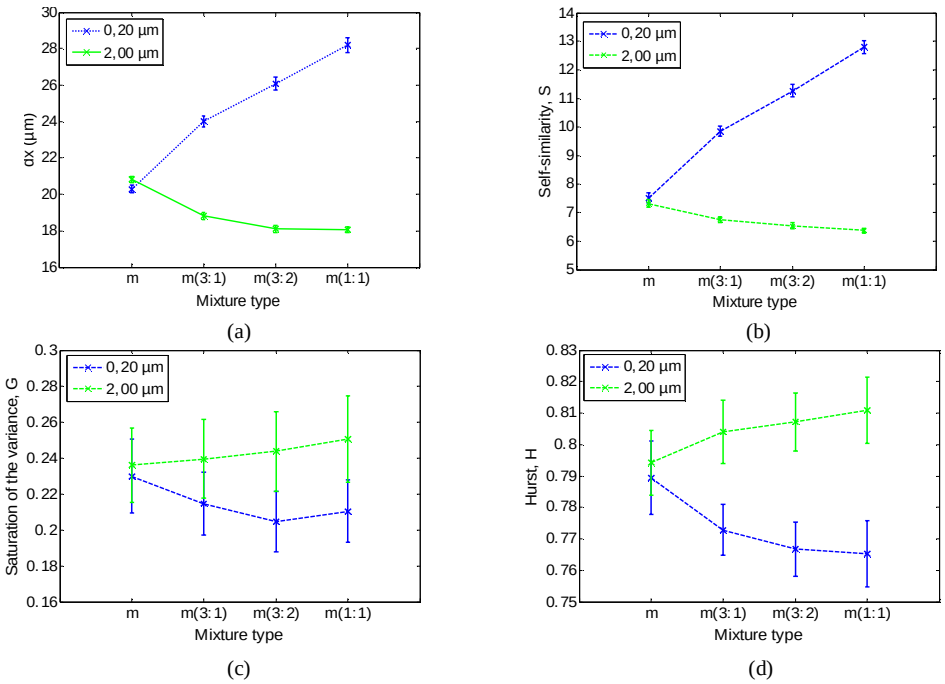

Fig. 7. Evolution of speckle size *dx* (a) and model parameters (Self-similarity *S* (b), Saturation of the variance *G* (c) and Hurst coefficient *H* (d)), versus microspheres size distribution. Mixture *m* corresponds to a mixture with a volume fraction f_v =1/6 for each microsphere size, mixture *m*(3:1), *m*(3:2) and *m(1:1)* correspond to the mixture *m* supplemented with smaller (0.20 µm) or larger microspheres (2.00 µm) with a ratio of (3:1), (3:2) and (1:1), respectively.

In the case of smaller microspheres addition (0.20 µm), the same statistic tests show discrimination, with a p-value less to 0.01, between all mixtures for *dx* and *S*. *H* discriminates all mixtures except mixtures *m*(3:2) and *m*(1:1). *G* does not discriminate mixtures *m*(3:1) and *m*(1:1). In the case of addition of larger microspheres (2.00 µm), all mixtures have been discriminated by *S* and *H*. Nevertheless, *G* does not discriminate mixtures *m* and *m*(3:1), and *dx* does not discriminate *m*(3:2) and *m*(1:1), as shown the same statistic tests used.

6. Discussions

6.1 Samples discrimination

In the case of monodisperse samples and according to the ANOVA test, the speckle fractal approach allows a better discrimination between microsphere diameters studied. Indeed, two parameters of the model, the Self-similarity *S*, and the Hurst coefficient *H*, discriminate all microsphere sizes studied with a p-value $p << 0.01$, contrary to speckle size which not discriminate 1.00, 1.50 and 2.00 µm.

In case of mixtures, *H* and *S* allow discrimination for all mixtures samples for larger microspheres addition, contrary to speckle size which does not allow discrimination for mixtures *m*(3:2) and *m*(1:1). For addition of smaller microspheres, we have discrimination between all mixtures for the Self-similarity *S*, and speckle size *dx* . Therefore, at least one of model parameters discriminate all mixtures in the two types of them, that is not the case of the speckle size which discriminates all mixtures only in case of addition of smaller microspheres.

Consequently, the speckle stochastic approach gives a better discrimination of our samples, under the used experimental conditions.

#84216 - $15.00 USD Received 18 Jun 2007; revised 1 Aug 2007; accepted 29 Aug 2007; published 5 Oct 2007

6.2 Parameters evolution

In Fig. 6(a), we can see that the speckle size decreases when the microsphere diameter increases with an exponential tendency. This speckle size behaviour with microspheres diameter was already observed in [11] in case of three different diameters (0.20, 1.44 and 3.17 µm) for μ_s = 140 cm^{-1}. We can see in Fig. 6(a) and Fig. 6(b) that the evolution of the Self-similarity parameter *S* with the microsphere diameter *d* is similar to the evolution of the speckle size. We observe the same similitude for mixtures [Fig. 7(a) and Fig. 7(b)]. This can be explained because S and *dx* are both related to a dimension at a local scale in the image: *dx* is a mean dimension of the grain width and *S* gives the dimension in the image of the self-similarity behaviour, which is in the grain neighborhood. We can observe that the addition of smaller scatterers in the mixture *m* increases these parameters and addition of larger scatterers decreases them. Once more, this is coherent for speckle size with [11] where they studied two mixtures in different volume fraction composed of two microsphere diameters at μ_s =140 cm^{-1}. We could expect these parameters behaviour when we add smaller or larger scatterers: the effect of a microsphere diameter type on the speckle parameters increases with its concentration in the mixture; therefore in case of smaller microspheres addition (respectively larger), these parameters increase (respectively decrease) and tend toward their maximum (respectively minimum) value observed in case of monodisperse sample.

We remark an increase tendency of Hurst coefficient, *H* with microsphere diameter [Fig. 6(d)] until a maximum at *d* = 1.50 µm. This behaviour seems similar to the scattering efficiency factor *Qs* and to the anisotropy coefficient *g* (see Table 1 and Fig. 8) where a maximum value is also observed at *d* = 1.50 µm. Therefore, Hurst coefficient, a local characteristic of the image, would seem to be related on characteristics of particles scattering. As for the experiment on monodisperse microspheres, in case of mixtures, *H* has an opposite evolution compared to the Self-similarity parameter: addition of smaller microspheres decreases *H* whereas addition of larger microspheres increases it [Fig. 7(d)]. Again, the more we add a microsphere diameter type, the more we have values near of those we had for monodisperse microspheres sample.

Saturation of the variance, *G* increases with microsphere diameters until one reaches values about the wavelength used, *i.e.* 0.75 µm. Beyond that, it is difficult to exploit.

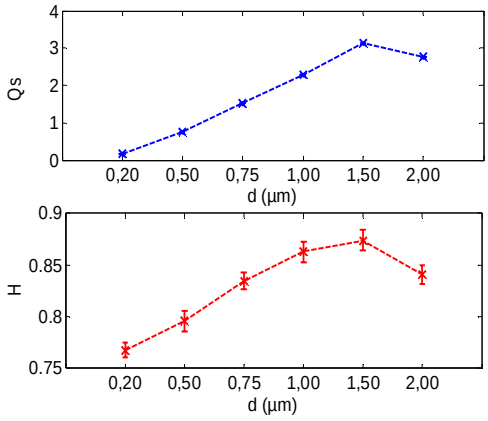

Fig. 8. Comparison of the evolution aspect of scattering efficiency factor, *Qs* and Hurst coefficient *H*, according to the microsphere size *d*.

The evolution of speckle size with scatter size can be explained as follow. According to the Van Cittert and Zernike theorem [7], in the case of surface illumination in reflection, the speckle size is inversely proportional to the dimension of the light spot responsible for the surface illumination. In the case of scattering media and by the application of this theorem, the

#84216 - $15.00 USD Received 18 Jun 2007; revised 1 Aug 2007; accepted 29 Aug 2007; published 5 Oct 2007

mean speckle size is determined by the surface of the backscattered spot *i.e.* the surface of the scattering volume seen by the CCD camera [32]. Particularly, authors in [11, 33] show a decrease of speckle size from solutions of monodisperse-sized polystyrene microspheres in backscattering configuration, with increasing g and μ_s that is in accord with our obtained results. As Self-similarity parameter and Hurst coefficient are both related to speckle grain, we can consider that their evolution with the changing scatterer size is caused by changes in angular distribution of backscattered light induced by the scatterer size change.

We have a different behaviour between the three model parameters for a given sample. This particularity would mean that these parameters are connected to different properties of the image. Moreover, according to Eq. (15), we can consider that model parameters constitute a mathematical parameterization of the autocorrelation function measured $c_I(x,0)$, that allow extraction of more parameters than the speckle size. Consequently, integrating the multi-scale aspect of the speckle pattern, model parameters would provide complementary information about the image and thus, about the medium.

7. Conclusions

In this paper, we presented an application of speckle statistical study on tissue phantoms through two approaches: a classical frequential approach through the speckle dimension measurement and a stochastic approach through the fractional Brownian motion approximation. For the last one, the autocorrelation function of the speckle pattern is modelized by the mathematical expression of Eq. (15). This approximation allows to extract three parameters [18]: the Hurst coefficient H, the Self-similar element S, and the Saturation of the variance G. These parameters characterize the image at three different scales.

We showed that these model parameters allowed to discriminate several media of tissue phantoms, consisting in monodisperse-polystyrene microspheres in solution of deionised water of different sizes and mixtures of them. Under used experimental conditions, these parameters allowed a better discrimination between our media than the speckle size as shown by the ANOVA test. Moreover, different behaviours between model parameters allowed different interpretations concerning their physical signification. Particularly, H seemed to be related on scattering properties of scatters, S and dx on dimension in the speckle pattern trough the size of its grains. The modelization of the speckle pattern by the fractional Brownian motion statistic allows the integration of the multi-scale aspect of the speckle, and therefore should provide more information about the scattering medium than the speckle size.

Currently, we are applying this method to discriminate *in vivo* several cutaneous pathologies. We hope to understand the optical signification of these model parameters by continuing to evaluate the relationship between their evolution and modifications in scattering media. We wish that speckle study becomes thus a non invasive tool aimed at helping diagnosis, which will be of great interest for dermatologists.

Acknowledgments

The authors thank DGA (Délégation Général de l'Armement) for their financial support.

#84216 - $15.00 USD Received 18 Jun 2007; revised 1 Aug 2007; accepted 29 Aug 2007; published 5 Oct 2007